Design of Dual Stopband Filters for Interference Suppression

Joaquin F. Valencia Sullca[#], Santiago Cogollos[#], Vicente E. Boria[#], Marco Guglielmi[#], Simone Bastioli[$], Richard Snyder[$]
[#]Instituto de Telecomunicaciones y Aplicaciones Multimedia iTEAM,
Universitat Politècnica de València, Spain
[$]RS Microwave Company Inc., USA
joavasu2@teleco.upv.es, {sancobo, vboria}@dcom.upv.es, marco.guglielmi@iteam.upv.es,
sbastioli@rsmicro.com, r.snyder@ieee.org

***Abstract*— When a broad band receiving system is co-located with high power emitters, receiver saturation is a major issue. Rejection of the local high power signals with minimal effect on the rest of the receiver passband is required. In this context, we present in this paper a method for providing two rejection bands (dual band rejection rather than dual passband) in a new and unique waveguide application. Cavity resonators are combined with resonant irises to provide a pair of relatively narrow rejection bands (at least 25 MHz wide) located within a wide passband, achieving at least 50 dB rejection while maintaining passband loss values to less than 1 dB. The filter structure that we propose is based on a simple modification of the traditional narrowband reject band filter. In this paper, we first describe the basic dual-band reject filter structure, and then we outline its design for a practical example. The paper is concluded with a comparison between simulations and measurements, showing very good agreement, thereby fully validating both the structure and the design procedure.**

***Keywords*— dual-band, narrow-band, reject band filter, resonant apertures.**

I. Introduction

In this paper, we discuss a method for achieving two narrow band regions of rejection within a passband covering 3.25 to 4.25 GHz. Each reject band region will comprise at least 25 MHz width, at the -50 dB rejection points. The scenario is one in which a broadband receiver covering the 3.25 to 4.25 GHz band is located close to high power radar systems (or perhaps is being jammed by adversaries in the area). The desired value of rejection is greater than -50 dB in the rejection bands. The target insertion loss in the pass-bands is less than 1 dB. Using the structure that we propose, it will be possible to design a filter that provides two narrow rejection bands, with a passband region between the rejection bands, in the frequency ranges of interest. As the method described utilizes waveguide technology, it is anticipated that higher power interfering signals will not cause harm to the filter network, or to the protected receiver. It should be noted that this contribution covers two reject bands. However, using a cascade of similar networks the number of rejection bands could be increased as needed.

The most classic implementation of a reject-band filter in rectangular waveguide is discussed in [1]. The structure is composed of a number of half-wavelength resonators connected to the top wall of a rectangular waveguide with capacitive irises that operate above cutoff. The resonators are separated from each other by a length of waveguide equal to multiples of one-quarter wavelength. Fig. 1 shows a typical structure with 5 resonators implementing 5 transmission zeros (TZs) in the frequency range of interest. The filter in Fig. 1, and all other filters discussed in this paper, are implemented using the WR-229 waveguide ($a = 58.166$ mm, $b = 29.083$ mm). Fig. 2 shows the simulated response of the structure in Fig. 1 (SRB Filter).

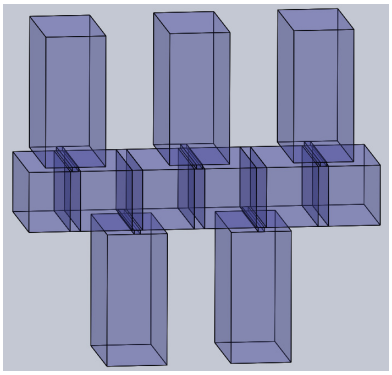

Fig. 1. Structure of the standard reject-band reference filter.

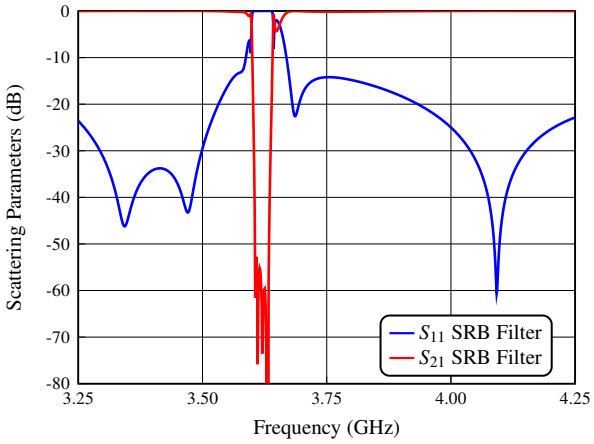

Fig. 2. Simulated performance of the standard reject-band reference filter.

As we can see in Fig. 2, the structure does provide a stop-band of about 55 dB. As expected, the rejected bandwidth is narrow, namely, from 3.606 GHz to 3.6322 GHz which is equal to about 26 MHz.

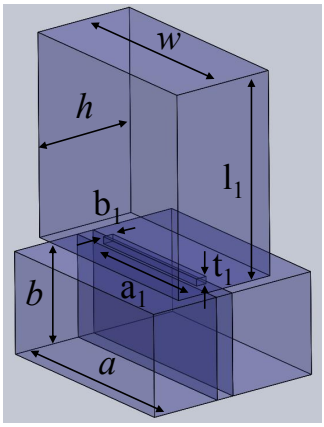

Fig. 3. Structure of the unit cell of the dual-band reject filter.

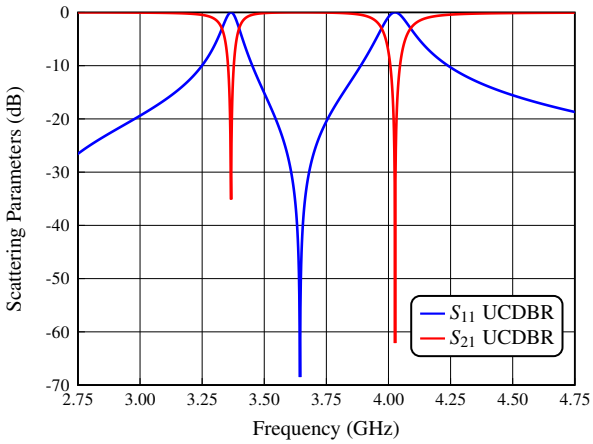

Fig. 4. Simulated performance of the unit cell of the dual-band reject filter.

II. Basic Dual-Band Reject Filter

The unit cell of the novel dual-band reject filter that we propose is shown in Fig. 3 (UCDBR). To implement the dual-band filter, we propose to decrease the width of the aperture connecting the main waveguide to the reject band resonator, to less than the a dimension of the main waveguide. This very simple change will allow the aperture to have a double function. Namely, at low frequency the aperture will be below cutoff and will have an inductive coupling behavior. However, as the frequency increases, the iris will eventually reach the cutoff frequency becoming a resonant aperture (RA), thus contributing an additional transmission zero (TZ). As the frequency is increased further, the aperture will behave as a normal capacitive iris. The dimensions of the UCDBR are as follows: the aperture is $a_1 = 39.00$ mm wide, $b_1 = 3.00$ mm high and $t_1 = 2.00$ mm thick, and the resonator is $w = 58.166$ mm wide, $h = 29.083$ mm high and $l_1 = 58.0$ mm long.

It is interesting to note that a similar approach to implement dual-band filters has already been demonstrated in [2], [3], in the context of dual-band bandpass filters. In this paper, the applicability of this simple concept is effectively extended to the implementation of dual-band reject filters.

To continue, we now provide a simple physical explanation of the behavior shown in Fig. 4, namely:

1) The frequency at which we have a reflection zero (RZ), is due to the fact that the short-circuited length of waveguide becomes exactly half-wavelength long, thus bypassing the effect of the RA. The resonant frequency of the RA has to be located near this point if we want a near-symmetric location of the TZs around the RZ.
2) The first TZ is due to the resonant aperture, which is below the resonance (therefore inductive in behavior), combined with the capacitive behavior of the waveguide length ($l_1 < \lambda_g/2$) thus producing the resonance and the TZ.
3) As we increase the frequency above the RZ, the RA has now capacitive character and the waveguide length is inductive ($l_1 > \lambda_g/2$), thus producing again a resonance that becomes the second TZ.

We have next investigated the relation between the structural parameters defined above and the position of the three main features of the structure, namely, the two TZs and the RZ. The results of our investigation (not included here for the sake of space) indicate that, although all structural parameters do influence the S_{21} parameter, it is indeed possible, using optimization, to change the frequency location of one of the features at the time while leaving the other two at the same frequency location. For instance, the independent control of the first TZ can be achieved moving a_1, and accommodating w and l_1 accordingly. The RZ can be shifted just moving w and recalculating a_1 and l_1. Finally, the second TZ can be controlled changing l_1, and slightly changing a_1 and w. Furthermore, our study indicates that the height b_1 of the RA affects the bandwidth of both reject bands at the same time. As a final remark, it is noticed that the two bands appearing in Fig. 4 have a slight asymmetry due to the dispersion of the waveguide. This fact will produce a slight difference in the bandwidth values of both rejection bands.

III. Design Example

One of the interesting features of the structure in Fig. 3 is that if we cascade a number of UCDBRs, the interaction between the various TZs is indeed not very strong. This allows for a very straightforward filter design procedure. It is, in fact, possible to start the design by defining first individual cells to produce TZs at the desired frequency locations. The various cells can then be cascaded, and an optimizer can finally be used to obtain the desired final performance.

Fig. 5 shows the structure of a five-pole dual-band reject filter (DBRB Filter) that we have designed as an application example. Fig. 6 shows the simulated behavior of the structure. As we can see from Fig. 6, we do obtain a rejection level that is greater than 57 dB, and, as expected, the rejection bandwidths are rather narrow, namely, only 53 MHz (lower) and 72 MHz (upper). Furthermore, the -1 dB passband between the rejection bands is about 332 MHz.

It is important to note at this point that all the waveguide structures that we have discussed so far have been simulated

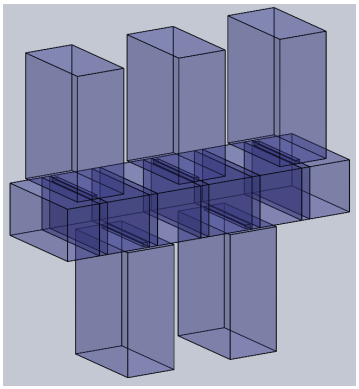

Fig. 5. Structure of the five-pole dual-band reject filter (narrow band).

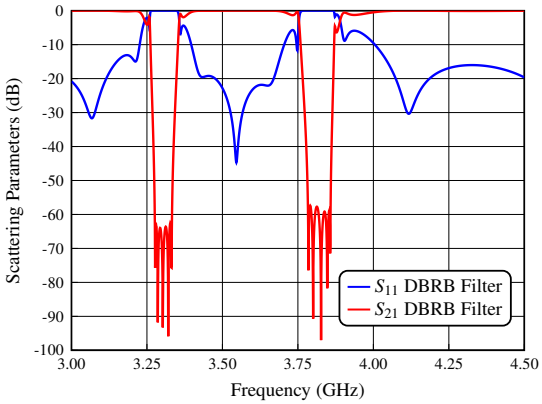

Fig. 6. Simulated performance of the five-pole dual-band reject filter (narrow band).

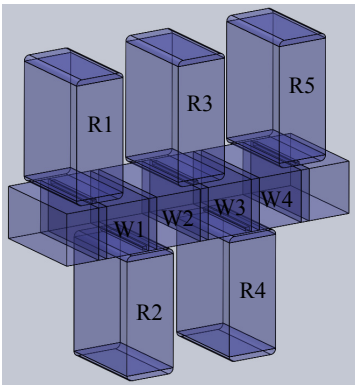

Fig. 7. Structure of the five-pole dual-band reject filter (narrow band) designed with radius equal to $r = 3$ mm in the vertical resonators.

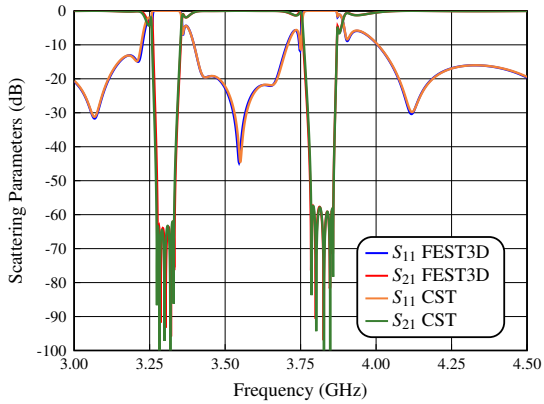

Fig. 8. Simulated performance of the five-pole dual-band reject filter (narrow band) using FEST3D (LA) and CST (HA).

with the commercial tool FEST3D in the low accuracy (LA) mode. However, in order to manufacture and measure a prototype, we now need to go from the LA to the HA (High Accuracy) simulation space.

The HA design has been carried out following a combination of [4] and the well-known aggressive space mapping (ASM) procedure [5], which requires the use of two different electromagnetic simulators. The first one is FEST3D, which is very fast when used with low-accuracy (LA) setting. The second is CST, which is an HA simulator but is time-consuming.

In addition, in order to facilitate manufacturing, the sharp corners of the vertical resonators have been changed into rounded corners with a radius equal to $r = 3$ mm. The resulting structure is shown in Fig. 7.

Fig. 8 shows a comparison of the simulated behavior of the dual-band structure obtained with the commercial tools: FEST3D and CST Studio Suite. As we can see, the agreement is very good.

Table 1 shows the final values for all dimensions of the dual-band reject filter. The thickness of the RAs is t_i.

IV. Hardware Measurements

Before manufacturing a prototype, we have carried out an analysis to evaluate the sensitivity of our design to manufacturing errors. The results of our analysis (not included here for the sake of space) indicate that an error lesser than ± 50 μm should be adequate. Furthermore, it is expected that the power handling capabilities of this filter are similar to the ones for a traditional single rejection band topology, since in both cases the critical points are located in the apertures and they are practically of the same size.

A prototype was therefore manufactured, in a clam-shell configuration, using a standard CNC process. Fig. 9 shows the prototype, while Figs. 10, 11 and 12 show a comparison between simulation and measurement results. Furthermore, the measured -1 dB passband is 331 MHz wide, and the minimum insertion loss in the center of the passband is 0.03 dB. As we can see, very good agreement has indeed been obtained.

V. Conclusion

In this paper, we have discussed a new approach to the design of dual-band reject filters in rectangular waveguide based on the use of resonant apertures. The dual-band performance has been obtained with a very simple modification of the classic narrow-band reject-band filter structure. Finally, a dual-band reject filter has been designed, fabricated and

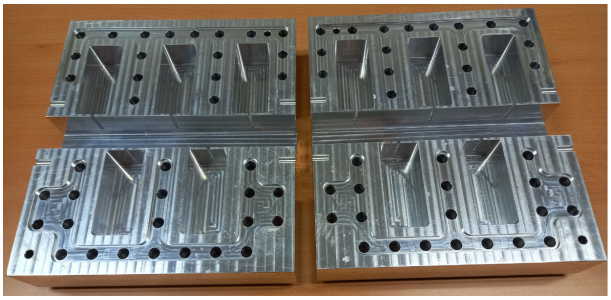

Fig. 9. Manufactured dual-band reject prototype in aluminum (no silver plating).

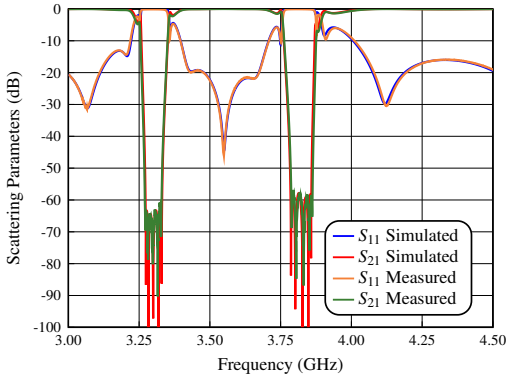

Fig. 10. Measurement of the performance of the dual-band reject filter compared with the EM simulation (CST).

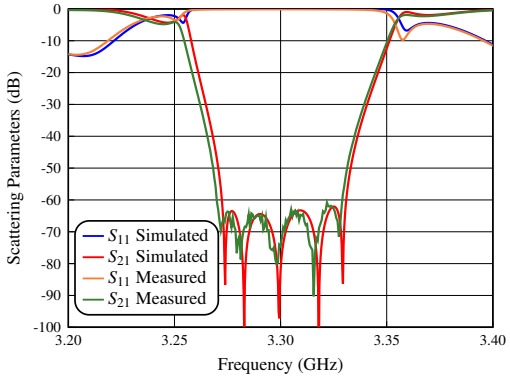

Fig. 11. Measurement of the performance of the dual-band reject filter compared with the EM simulation (CST) for the lower reject band.

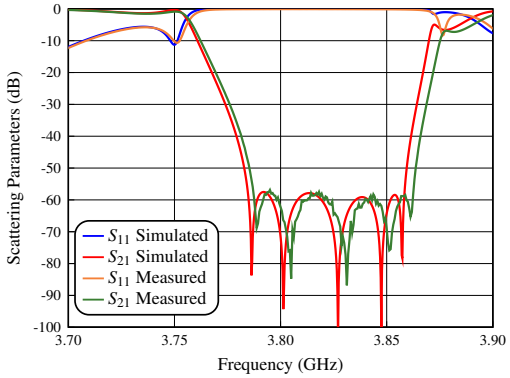

Fig. 12. Measurement of the performance of the dual-band reject filter compared with the EM simulation (CST) for the upper reject band.

Table 1. Physical dimensions for the dual-band reject filter.

Section Type	Dimensions all in mm	
Input Waveguide	a =58.17 b =29.083 $L_{input} = L_{output}$ =35	
Resonant aperture 1-5	a_1 =41.243 b_1 =2.500 t_1 =2.000	a_5 =42.015 b_5 =2.500 t_5 =2.000
Resonator 1-5	w_1 =52.434 h_1 =29.083 l_{1_1} =70.021	w_5 =52.599 h_5 =29.083 l_{1_5} =70.916
Waveguide 1-4	W_1 =58.170 H_1 =29.083 L_1 =29.037	W_4 =58.170 H_4 =29.083 L_4 =28.715
Resonant aperture 2-4	a_2 =42.010 b_2 =2.500 t_2 =2.000	a_4 =42.149 b_4 =2.500 t_4 =2.000
Resonator 2-4	w_2 =52.875 h_2 =29.083 l_{1_2} =69.514	w_4 =52.578 h_4 =29.083 l_{1_4} =69.438
Waveguide 2-3	W_2 =58.170 H_2 =29.083 L_2 =29.725	W_3 =58.170 H_3 =29.083 L_3 =29.705
Resonant aperture 3	a_3 =41.664 b_3 =2.500 t_3 =2.000	
Resonator 3	w_3 =52.419 h_3 =29.083 l_{1_3} =70.291	

measured, showing an excellent agreement between simulation and measurement, thereby fully validating both the structure and the design procedure.

ACKNOWLEDGMENT

This work was supported by Ministerio de Ciencia e Innovación (MICIN, Spanish Government) under R&D project PID2019-103982RB-C41 (funded by MICIN/AEI/10.13039/501100011033).

REFERENCES

[1] L. Young, G.L. Matthaei, and E.M.T. Jones, "Microwave band-stop filters with narrow stop bands," *IRE Transactions on Microwave Theory and Techniques*, vol. 10, no. 6, pp. 416–427, Nov. 1962.

[2] J.F. Valencia Sullca, S. Cogollos, M. Guglielmi, and V.E. Boria, "Dual-band filters in rectangular waveguide based on resonant apertures," in *2021 IEEE MTT-S International Microwave Symposium (IMS)*, Jun. 2021, pp. 192–195.

[3] J.F. Valencia Sullca, S. Cogollos, V.E. Boria, and M. Guglielmi, "Compact dual-band and wideband filters with resonant apertures in rectangular waveguide," *IEEE Transactions on Microwave Theory and Techniques*, vol. 70, no. 6, pp. 3125–3140, Jun. 2022.

[4] M. Guglielmi and A. A. Melcon, "Novel design procedure for microwave filters," in *1993 23rd European Microwave Conference*, 1993, pp. 212–213.

[5] J. Bandler, R. Biernacki, S. H. Chen, R. Hemmers, and K. Madsen, "Electromagnetic optimization exploiting aggressive space mapping," *IEEE Transactions on Microwave Theory and Techniques*, vol. 43, no. 12, pp. 2874–2882, Dec. 1995.